Title: The determination of a 3D length scale using long reconstructed fiber paths

Authors (names are for example only): Mathew Schey
Scott E. Stapleton

Paper Number: **114**

Mathew Schey and Scott Stapleton, Dept. of Mechanical Engineering, University of Massachusetts Lowell, 1 University Avenue, Lowell, MA 01854, U.S.A.

(FIRST PAGE OF ARTICLE)

ABSTRACT

Carbon fiber reinforced composites often exhibit large amounts of property scatter. Attempts at understanding composite property scatter have led researchers to generate many 2D models which ignore the 3D phenomenon of entanglement. Previous studies of entanglement have suggested it is correlated to a length scale, but have not had large enough samples to determine its size. In this study, fiber paths of long, entangled, continuous fibers were extracted from CT data of an automotive grade, heavy tow composite. Descriptive metrics of these fiber paths were used to quantify the entanglement as a function of position along the fiber direction. Using this data, several minimum length scales for capturing the behavior of multiple descriptors were determined. These length scales revealed where statistical representation of 3D fiber models provides superior information to that of 2D models.

INTRODUCTION

Carbon fiber reinforced composites have become the material of choice for many applications due to their high strength to weight ratios. One of the keys to understanding these materials involves the study of the microstructure of the composite. Modeling such materials has often been done using 2D ideal fiber models, where fibers are spaced perfectly and assumed to be parallel. It has long been observed, however, that the variability of the microstructure leads to scattering in the properties and performance of CFRPs. Fiber meandering and entanglement, for example, is thought to be directly related to resin distribution, crack formation, and the failure potential of the sample. Random 2D representative volume elements (RVEs) were created to depict realistic fiber arrangements more accurately [1], [2]. The results of these analyses have shown that the arrangement and volume fraction has a significant affect to the transverse

---

Mathew Schey and Scott Stapleton, Dept. of Mechanical Engineering, University of Massachusetts Lowell, 1 University Avenue, Lowell, MA 01854, U.S.A.

properties of the composite due to the introduction of stress concentrations [3], [4]. While the analysis of 2D RVEs has contributed greatly to research of the potential effects of fiber arrangements, they have failed to capture the entanglement that occurs within real world composites. Entanglement is a phenomenon which occurs when fibers inside a composite become intertwined, however severely. Previous works have studied the effects of entanglement using geometric and spatial descriptors which give insight into the changes in distribution and orientation of the fibers [5], [6]. In Fast et al. [5], it was hypothesized that there is a length scale associated with these metrics axially (in the fiber direction of a UD composite). While UD fiber models have been generated from μCT data at the fiber scale in the past, most of these models have not included any mention of these length scales as a function of descriptive metrics [6]. Furthermore, the μCT data used in both the determination of these length scales and modeling attempts was shorter than the length scales themselves, forcing researchers to estimate what the actual size of a UD fiber model of real fiber paths would need to be.

The scope of this work is to apply descriptive metrics which give insight into the entanglement within a CFRP of a long, continuous fiber composite. In this work, fiber paths were extracted from seven sequential synchrotron scans of an automotive grade, carbon fiber reinforced composite manufactured using VARTM. These paths were then stitched together to create continuous fiber paths the length of the seven scanned segments (~4.5mm). The last cross-section in each set of images was correlated to the first section in the next set of images by finding the translation of the fiber paths which minimized the difference between each fiber's respective location. Entanglement was then quantified using a series of metrics which describe the spatial variation in density, angular orientation, and relative fiber interactions through the thickness of the sample were then applied. Using these metrics, a minimum length scale through the thickness of the sample was determined by studying the average, standard deviation, and kurtosis of the distribution of the metric as a function of scan length. Pearson's Correlation Coefficient, R, was also calculated to find the minimum distance at which a metric becomes decorrelated. For each fiber the associated values of each metric were correlated to the position along the fiber at which the value occurred. When R dropped below a certain threshold value the metric was deemed to be uncorrelated with position along the fiber's length. With the determination of this length scale, more accurate modeling of entangled fiber reinforced composites may be achievable.

METHOD

An automotive grade heavy tow composite was scanned in seven sequential scan sets using a synchrotron. Fiber paths were extracted from the scans using a custom software in MATLAB. These fiber paths were then manually stitched together to make a sample seven times the length of any single scan set. A series of metrics were then used to quantify the longer sample.

Materials

For this study, scans of an automotive grade, fiber-reinforced composite were compared, an aerospace- and automotive grade composite. The composite was manufactured at the Institute for Textile Technology at RWTH Aachen University from Toho Tenax STS40 F13 48k tows. Each tow contained 48,000 fibers, which decreases the cost of the carbon fiber due to bulk manufacturing. The tows were infiltrated with Hexion Epikote RIMR 135 with an Epikure RIMH curing agent. The tow was infiltrated using VARTM at a pressure of 1000 mbar.

Image Procedure and Analysis

All seven automotive-grade scan sets were scanned from the same heavy-tow composite at the European Synchrotron Radiation Facility (Figure 1). Scans were taken at a resolution of 0.332 μm/voxel, with 2048 pixels in the fiber direction and 2098 pixels in the transverse directions. To reduce the computational load, every third image was analyzed in the stack of automotive scans, resulting in a total of 4774 images with spacing of 0.996 μm between images (4755 μm in total length). The high energy levels used in the synchrotron process produced images which contained high fiber to matrix contrast.

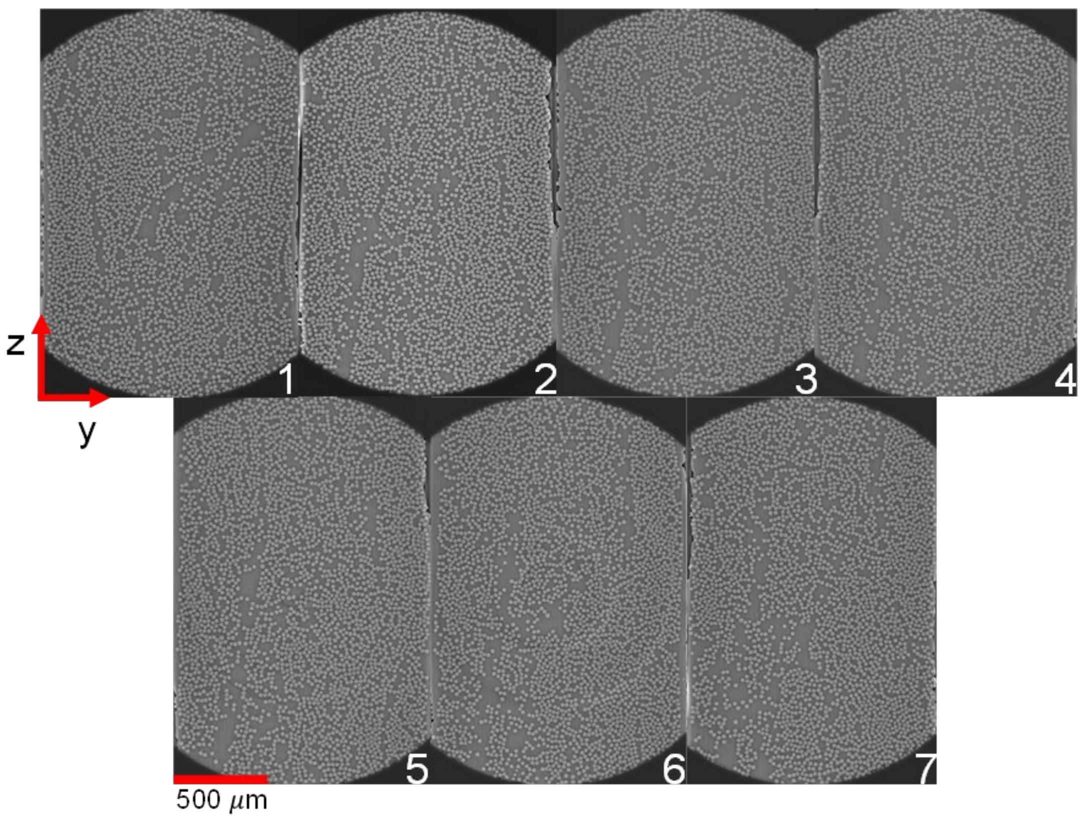

Figure 1. First cross-section from all seven scanned sections of the automotive grade heavy to composite scanned using a synchrotron

One of the major challenges with analyzing all seven scan sets was that the scan sets themselves were not aligned perfectly. Uncorrected, this would make the process of detecting and correlating individual fiber paths from one scan to another impossible. The solution for this issue was to first detect fiber paths in each individual scan set and reconstruct them. Fiber paths were detected using MATLAB's built-in "imfindcircles" function, which uses a circular Hough transform to detect the center and outline of circular objects within images. After all circles were detected, a nearest neighbor search was performed within the data set to correlate a fiber's position in one cross-section to its position in another [7]. The assumption employed here was that the stiffness of the fibers and the relatively short intra-scan distance would not permit large deviations in fiber position from one scan to the next.

After all fiber paths were extracted from the seven scanned sections, the first two sets of fiber paths were manually stitched together by correlating the fiber positions from the last cross-section of the first scan set to those of the first cross-section of the second set. Fibers were correlated to one another by looking at unique fiber groupings which are easily recognizable from one cross-section to the next. At first, only one distinct fiber group was used to find the translation vector between scan set 1 and scan set 2. After translating the coordinates of set 2 to line up with set 1 it was observed that there was a small offset remaining between the two fiber sets. Upon further investigation, it was discovered that this offset could be reduced by using more than one fiber grouping to obtain the correct translation vector. In the end, three translation vectors were found using three fiber groupings, and averaged together. This led to the least amount of offset over all fibers. This process was then repeated five more times for the five remaining connections. In the end, a total of 2591 fiber paths remained, all of which spanned an axial length of 4.76 cm.

Metrics

Spatial fiber metrics were measured from the extracted fiber paths to observe the effects of debulking on each sample.

LOCAL FIBER VOLUME FRACTION

The local volume fraction, v_f^i, is the ratio of a fiber's cross-sectional area to the area of that fiber's Voronoi cell in a cross-section (Figure 2). Unlike the global volume fraction, the local metric provides information on localized regions of high fiber density or sparsity within the sample. The local volume fraction (Equation 1) can be calculated as

$$v_f^i(x_n) = \frac{\pi r^2}{A_v^i(x_n)} \tag{1}$$

where r is the average fiber radius of all fibers and $A_v^i(x_n)$ is the area of the Voronoi cell of fiber i at the cross-section x_n.

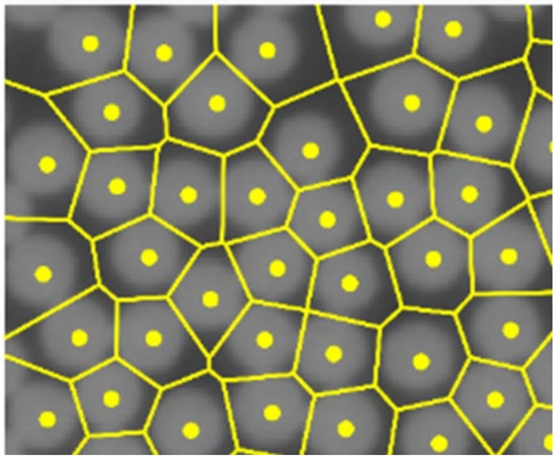

Figure 2. Cropped section of a CT image showing the Voronoi tessellation of the fiber centers used to calculate the local volume fraction, v_f^i, of each fiber

LINEAR POLAR ANGLE

The linear polar angle, $\overline{\gamma}$, of a fiber is a measure of the magnitude of a fiber's angular deviation from its intended manufactured direction (Figure 3). The process of calculating $\overline{\gamma}$ starts with first linearizing each fiber path by its best linear approximation in 3D. Once linearized, $\overline{\gamma}$ is the max angle of the linearized fiber from the x-axis measured in any direction. The linear polar angle can be calculated as

$$\overline{\gamma_i} = \cos^{-1} \frac{x_i(n)}{S_i} \, where \, n = 1:N \tag{2}$$

Where $x(n)$ is the axial location in the sample at the n^{th} cross-section, and S_i is the length of the linearized fiber i, and N is the final cross-section. For the purposes of this paper, the variable n will be varied from one the N so that the influence of length axially on this metric can be studied.

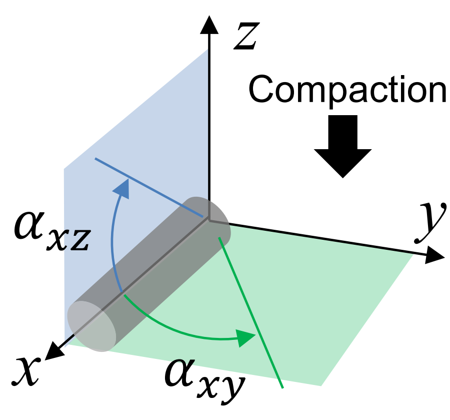

Figure 3. Diagram of a fiber showing the xz and xy planes in which the linear polar angle is calculated from

RESULTS AND DISCUSSION

LOCAL FIBER VOLUME FRACTION

The local fiber volume fraction is a measure of the spatial variations in density of fibers in a particular cross-section of a fiber reinforced composite. The local fiber volume fraction distribution for all cross-sections is shown in Figure 4. The average local fiber volume fraction for the sample was calculated to be 0.48 with a standard deviation of 0.102. While the distribution of the metrics like the local volume fraction provides information on the global sample (all seven stitched scan volumes), it does not provide much information on how this metric varies as a function of scan length. To shed more insight on this, a length scale analysis was performed.

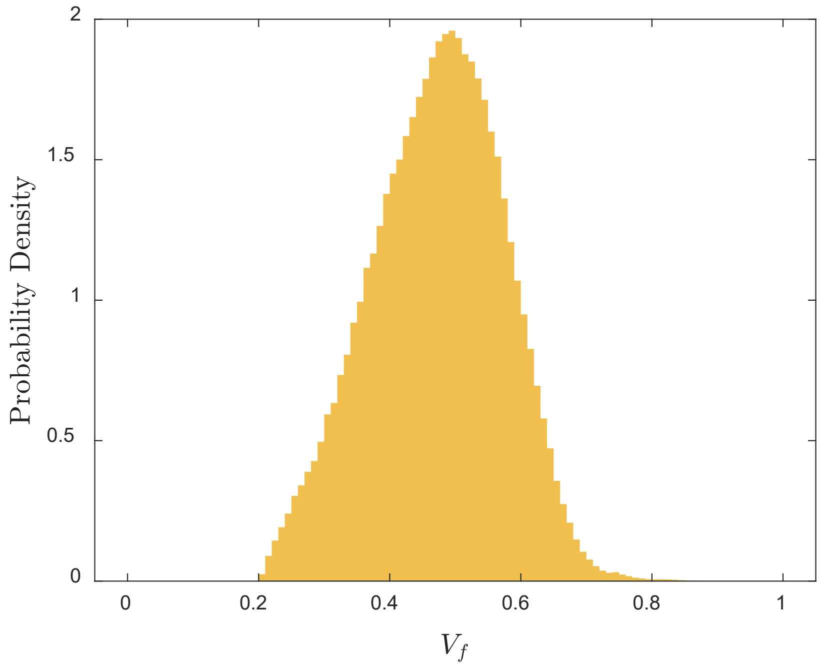

Figure 4. Distribution of local fiber volume fraction, v_f, of all fibers in all cross-sections

To perform the length scale analysis the length of the sample was varied by iteratively adding an additional cross-section each step. Every time a cross-section was added to the sample, all metrics were recalculated and stored in an array containing the results from the previous steps. In the end this produced an array of data which showed the results of each metric as a function of the length of the scanned volume in which they were measured. Using this data, the average, standard deviation, and kurtosis of the entire sample as a function of the length of the scanned volume were calculated for each metric. Additionally, Pearson's Correlation Coefficient was calculated for each metric as a function of the length of the scanned volume.

Results of the length scale analysis using the local volume fraction are shown in Figure 5a-d. Results for both the average local fiber volume fraction and the standard deviation of the average local fiber volume fraction show little to no change in this metric as the scan length is increased (Figure 5a-b). This suggest that, for local fiber volume fraction, a 2D RVE (no length) is a good predictor of the average and variance of this metric. The standard deviation, while consistent, is high when compared to the mean of the data. This fact, together with how consistent the mean local volume fraction is, highlights the fact that the scanned volume is essentially a closed volume. The number of fibers analyzed in the sample is the same in every cross-section, meaning that the mean local fiber volume fraction cannot vary very much. At the same time the standard deviation of the local fiber volume fraction remains high, meaning that any fibers which reorient themselves towards less fiber-dense regions also leave space for once sparse fibers to reorient themselves towards denser regions. The kurtosis, however, shows that a 2D RVE fails to accurately capture the presence of outlier fibers for this metric (Figure 5c). The kurtosis of this metric does not level out until a scan length of 2000 μm, after which it remains consistent.

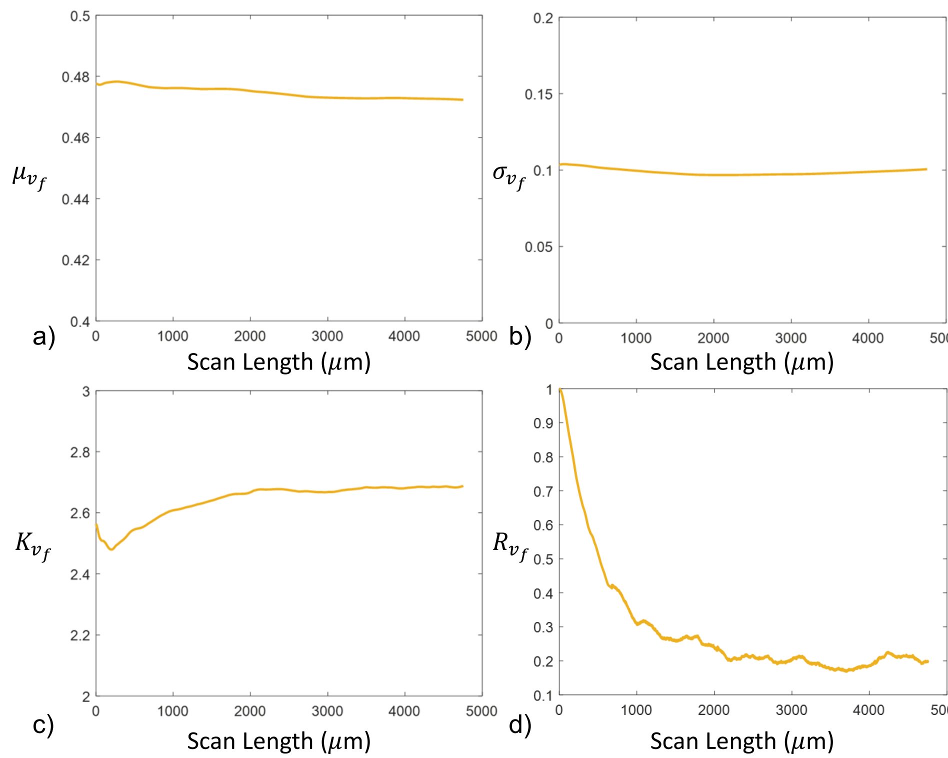

Figure 5. Length scale analysis of the local fiber volume fraction, v_f, showing a) the average v_f, b) the standard deviation of v_f, c) the kurtosis of v_f, and d) Pearson's Correlation Coefficient of v_f as the scan length is increased

The correlation length for a metric is defined as the scan length at which Pearson's Correlation Coefficient falls under a value of 0.5. This value represents the length at which measurements of that metric can no longer be correlated to the values of that metric in the first cross-section. In the case of the local volume fraction this value represents the length at which the spatial variation in density of the fibers, and consequently the fiber positions themselves relative to one another, are no longer related in any way to the spatial density of the fibers in the first cross-section. The scan length at which this occurs is 560 μm, which is shorter than any one of the 7 stitched scan volume (682 μm).

FIBER LINEAR POLAR ANGLE

The linear polar angle is a measure of a fiber's max deviation from the axial direction of the composite. The average polar angle was calculated to be 0.8929 degrees, with a standard deviation of 0.6346 degrees. Given that the linear polar angle is calculated using the best linear approximations of each fiber path, the nature of this metric is inherently that of a geometric descriptor instead of a spatial one like the local volume fraction.

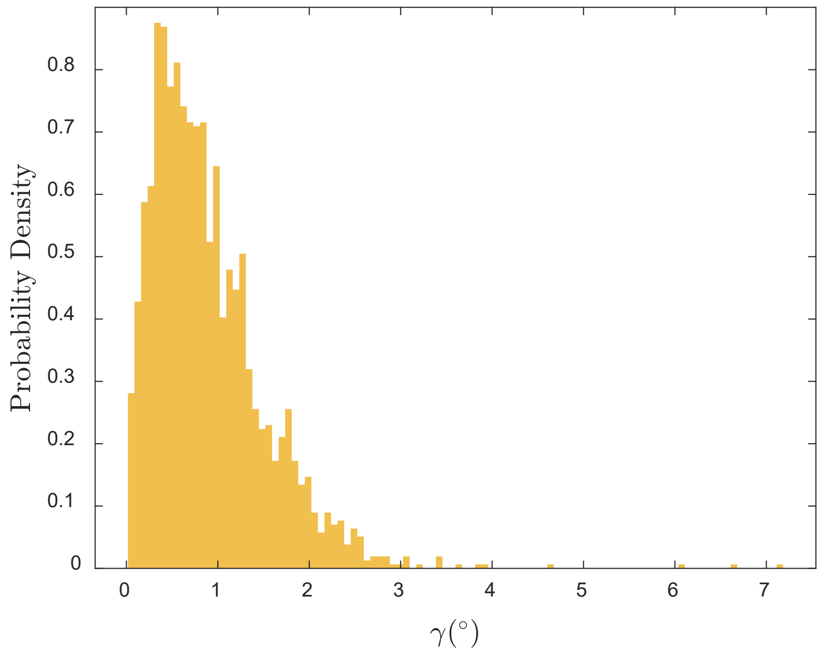

Figure 6. Linear Polar Angle distribution for all fibers

Results for the length scale analysis of the linear polar angle are shown Figure 7a-d. The mean linear polar angle decreases as the scan length increases, from 1.6 degrees to 1.25 degrees at the final scan length (Figure 7a). The standard deviation shows a similar trend as the mean, decreasing from 1.05 degrees to 0.85 degrees (Figure 7b). The standard deviation of the linear polar angle remains very high when compared to the mean suggesting the fibers don't exactly have one true direction that they're oriented in. The kurtosis of the linear polar angle increases as the scan length increases, meaning that the number of outlier fibers with respect to orientation increases as the sample gets longer. Given that the individual fibers themselves do not change this could indicate that certain fibers become more curved as the scan length increases.

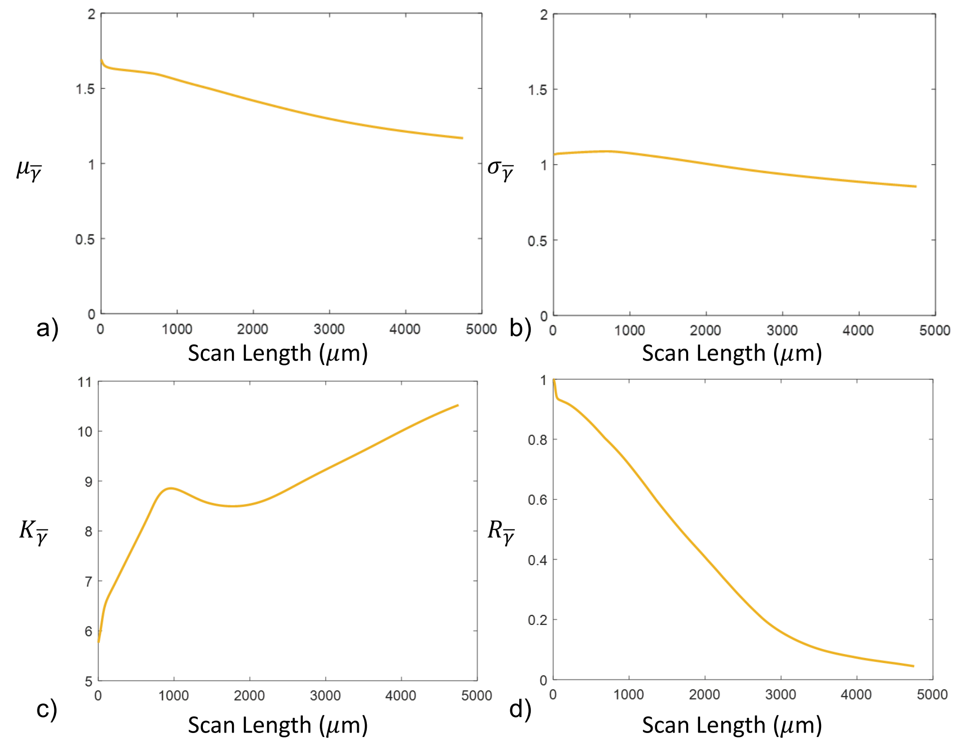

Figure 7. Length scale analysis of the linear polar angle, $\overline{\gamma}$, showing a) the average $\overline{\gamma}$, b) the standard deviation of $\overline{\gamma}$, c) the kurtosis of $\overline{\gamma}$, and d) Pearson's Correlation Coefficient of $\overline{\gamma}$ as the scan length is increased

The correlation length of the linear polar angle was found to be 1663 μm, which is well over twice the size of one of the 7 scanned sections and over three times the size of the correlation length for the linear polar angle. In the case of the linear polar angle, a metric which is calculated using the best linear approximation of each fiber, the correlation length is a measure of both when the misorientation of the fibers become uncorrelated as well as when the linear approximation of the fibers breaks down. This could potentially occur due to fiber becoming more curved with increased scan length, as was hypothesized with the increase in kurtosis.

SUMMARY AND CONCLUSIONS

An automotive grade, heavy tow composite was imaged into seven scan sets using a synchrotron. Fiber paths from each of the scans were extracted and stitched together to make long, continuous fiber paths the length of all seven scan sets. Two descriptive metrics were then calculated which describe the spatial density of the fibers as well as their orientation. These metrics were then recalculated as the scan length of the sample was constantly increased. The results of each metric were recorded after each successive new cross-section was added. The mean, standard deviation, kurtosis, and Pearson's correlation coefficient, *R*, were then calculated for the data. Using this data the minimum scan length at which these metrics could be fully captured was determined.

The results for the local volume fraction analysis show that the overall average local volume fraction for all seven stitched samples was 0.48, with a standard deviation of 0.102. The standard deviation is relatively large when compared to the mean for this metric, meaning that the microstructure itself is spatially organized non-uniformly in terms of fiber packing. While this information may be valuable in terms of characterizing the microstructure, it provides little information on what size would be needed to accurately model this microstructure in 3D. The length scale analysis, however, showed that the mean and standard deviation of the local fiber volume fraction does not vary significantly as a function of increased scan length. This means that a representative model for this microstructure could be made in the form of a 2D RVE if the goal of the model was to understand a link between mean and standard deviation of spatial fiber density and, for example, axial strength of a composite. The kurtosis and correlation length, however, show a much different story. The kurtosis of the local fiber volume fraction does not plateau until ~2000 μm in the fiber direction, meaning that the fibers in the distribution of this metric are not fully captured until this length. Outliers, in this context, represent those fibers which are positioned such that they are very close to their surrounding nearest neighbor fibers (as in fiber clusters) or those which are oriented far from any other fibers (as in matric rich regions). Axially, a fiber's orientation may be such that its local fiber volume fraction may be an outlier value in one cross-section and near the mean of the distribution in another. This means that a fiber's position in one cross-section may make a stress concentrator, while its position in another cross-section may not show this fact at all. Therefore, to better understand failure initiation on the microstructural level an outlier-associated length scale (~2000 μm axially) may be necessary. Finally, the correlation length of the local fiber volume fraction was found to be 560 μm. The correlation length is a measure of the distance along the fiber direction in which measurements of the local fiber volume fraction can no longer be said to be correlated to the observance of these measurements in the first cross-section. Therefore, if the goal of a 3D model of this microstructure was to capture a volume in which all cross-sections followed the same trend in fiber density measurements it would need to be at least 560 μm in length.

Unlike the local fiber volume fraction, measurements of the average and standard deviation of the linear polar angle do not remain consistent as the scan length is increased. The kurtosis of the distribution increases rapidly as the scan length is increased. This suggests one of two things: the length of the scanned volume is not long enough to accurately capture the true mean and standard deviation of the microstructure, or the linear approximation of the fibers breaks down as more scan length is considered. Further analysis is required to understand which of the two is most responsible of the lack of convergence. The correlation length for this metric was calculated to be 1663 μm, which is the minimum length at which measurements of the linear polar angle can no longer be correlated to the measurements between the first two cross-sections. Worth noting here is that the kurtosis began to change its trend around a similar point in the sample, suggesting that the cause for decorrelation of this metric may be related to an increase in curvature of the fibers.

ACKNOWLEDGEMENTS

This work is based upon work supported by the National Science Foundation and Air Force Office of Scientific Research under grant number IIP1826232. Any opinions, findings, and conclusions or recommendations expressed in this material are those of the author(s) and do not necessarily reflect the views of the National Science Foundation.

REFERENCES

[1] A. Wongsto and S. Li, "Micromechanical FE analysis of UD fibre-reinforced composites with fibres distributed at random over the transverse cross-section," *Composites Part A: Applied Science and Manufacturing*, vol. 36, no. 9, pp. 1246–1266, Sep. 2005, doi: 10.1016/j.compositesa.2005.01.010.

[2] S. H. R. Sanei and R. S. Fertig, "Uncorrelated volume element for stochastic modeling of microstructures based on local fiber volume fraction variation," *Composites Science and Technology*, vol. 117, pp. 191–198, Sep. 2015, doi: 10.1016/j.compscitech.2015.06.010.

[3] Y. Swolfs, L. Gorbatikh, and I. Verpoest, "Stress concentrations in hybrid unidirectional fibre-reinforced composites with random fibre packings," *Composites Science and Technology*, vol. 85, pp. 10–16, Aug. 2013, doi: 10.1016/j.compscitech.2013.05.013.

[4] B. Fedulov, F. Antonov, A. Safonov, A. Ushakov, and S. Lomov, "Influence of fibre misalignment and voids on composite laminate strength," *Journal of Composite Materials*, vol. 49, no. 23, pp. 2887–2896, Sep. 2015, doi: 10.1177/0021998314557533.

[5] T. Fast, A. E. Scott, H. A. Bale, and B. N. Cox, "Topological and Euclidean metrics reveal spatially nonuniform structure in the entanglement of stochastic fiber bundles," *J Mater Sci*, vol. 50, no. 6, pp. 2370–2398, Mar. 2015, doi: 10.1007/s10853-014-8766-2.

[6] M. W. Czabaj, M. L. Riccio, and W. W. Whitacre, "Numerical reconstruction of graphite/epoxy composite microstructure based on sub-micron resolution X-ray computed tomography," *Composites Science and Technology*, vol. 105, pp. 174–182, Dec. 2014, doi: 10.1016/j.compscitech.2014.10.017.

[7] M. J. Schey *et al.*, "Identification and Quantification of 3D Fiber Clusters in Fiber-Reinforced Composite Materials," *JOM*, vol. 73, no. 7, pp. 2129–2142, Jul. 2021, doi: 10.1007/s11837-021-04703-0.